Multimode Interference 3dB splitters in hollow core metallic waveguides for low loss THz wave transmission

C. Markides, C. Themistos, H. Tanvir, B.M.A. Rahman, *Senior Member IEEE* and K.T.V. Grattan

***Abstract*—A multimode interference half-power splitter on hollow core polysterene-coated metallic waveguide is demonstrated in the present work. The modal properties, propagation length, optical field evolution and dispersion of the above device have been investigated using the full vectorial finite element-based modal analysis and beam propagation method, as well as the finite difference time domain approach.**

***Index Terms*—Finite Element Methods, Finite Difference Methods, Optical Waveguides, couplers**

I. Introduction

The terahertz (THz) region defined as the band from 0.1 to 10 THz. has attracted a lot of interest, because it offers significant scientific and technological potential for applications in many fields, such as in sensing [1], in imaging [2] and in spectroscopy [3]. Waveguiding in this intermediate spectral region is a major challenge due tor recent progress in sources [4] and receivers of THz waves. Various THz waveguides have been suggested, such as metallic waveguides [5], pipe-waveguides [6] and polymer-based fibers [7]. More recently, dielectric-lined hollow cylindrical metallic waveguides [8] and hollow-core plasmonic waveguides [9] have been presented, exhibiting very low transmission losses.

Multimode Interference (MMI)-based devices have been established for use in several wavelength-division multiplexing (WDM) systems, such as power splitters [10], and phased-array de-multiplexers [11] and balanced coherent receivers [12], due to the ease of fabrication, compactness, low-loss, wide bandwidth and low polarization dependence. MMI devices are based on the self-imaging property [13], where the guided modes of a multimode waveguide are excited and interfere constructively to produce single or multiple images of an input field launched usually via single mode optical waveguides at the one end of the structure, at periodic intervals along the direction of propagation. The number of the modes excited in each MMI structure and consequently the position of the images along the direction of propagation are dependent on the position of the input waveguides in the lateral *x*-direction, called the interference mechanism [13]. Under the symmetric interference (SI) mechanism, the first image of an input field launched via an input waveguide placed in the centre of the MMI width, is obtained at a self image length of $L_i=3L_\pi/4$, along the direction of propagation, where the coupling length, L_π, is defined by:

$$L_\pi = \frac{\pi}{\beta_0 - \beta_1} \tag{1}$$

where β_0 and β_1 are the propagation constants of the fundamental and the first higher order modes, respectively.

In the present work, a multimode interference half-power splitter is presented, based on the low loss hollow-core polysterene-coated plasmonic waveguide structure, for THz wave transmission.

II. Numerical Analysis

The Finite Element Method (FEM) [14] has been established as one of the most powerful numerical techniques, because of its accuracy, flexibility and versatility in the numerical analysis of optical waveguides, particularly in structures with arbitrary shapes, index profiles, nonlinearities and anisotropies. In the present work the full vectorial H-field finite element formulation with the aid of perturbation technique [15] has been applied for the modal analysis of the plasmonic waveguide structure, to determine the propagation characteristics of the fundamental and the first higher order mode and to estimate the MMI length using (1).

The BPM approach based on the paraxial wave equation [16] is widely used for the study of lightwaves in integrated optical waveguides. The Finite Element-BPM (FE-BPM) based on the Crank-Nicholson algorithm [18], incorporating

Manuscript received April 1, 2012.

C. Markides is with the Department of Engineering and Applied Sciences, Frederick University, Nicosia 1036, Cyprus (c.markides@cmarkides.info)

C. Themistos is with the Department of Engineering and Applied Sciences, Frederick University (phone: +357-22-431355; fax: +357-22-438234; e-mail: c.themistos@cytanet.com.cy).

H. Tanvir is with the Department of Engineering and Mathematical Sciences, City University, London, EC1V 0HB, UK (e-mail: H.Tanvir@city.ac.uk).

B.M.A. Rahman is with the Department of Engineering and Mathematical Sciences, City University, London, EC1V 0HB, UK (e-mail: H.Tanvir@city.ac.uk)

K.T.V. Grattan is with the Department of Engineering and Mathematical Sciences, City University, London, EC1V 0HB, UK (e-mail: K.T.V.Grattan@city.ac.uk)

the perfectly matched layer (PML) boundary condition [19] to absorb the unwanted radiation out of the computational domain has been used in the present work, providing an effective numerical tool for the analysis of the devices examined, since it utilizes all the advantages of the FEM. The BPM algorithm simulates the evolution of the optical power along the direction of propagation and due to the discretization of the device, the optical properties can be calculated for any transverse cross section of the structure at any position along the direction of propagation.

The two-dimensional finite-difference time-domain (2D FDTD) has been widely used as a highly efficient and versatile method for solving Maxwell's equations [20]. The FDTD method solves Maxwell's equations by first discretizing the problem space into rectangular cells and through explicit iterations applies finite-difference approximation to seek a direct solution to the time-dependent curl equations numerically. Since the FDTD method is an explicit scheme, there is a limit on the time step Δt to ensure stability in the algorithm,

$$S = c \cdot \Delta t \sqrt{\frac{1}{(\Delta x)^2} + \frac{1}{(\Delta y)^2}} \qquad (2)$$

where $S < 1$ and c is the wave propagation speed for the two-dimensional FDTD case. The stability factor ensures that the maximum time-step size is determined by the size of the cells in the *x*-, and *y*-direction in the computational domain. In simulating the multimode interference waveguide using the 2D FDTD method Perfectly Matched Layer (PML) [21] absorbing boundary conditions (ABC) are applied to terminate the problem space. In the present work the FDTD approach has been used to simulate the MMI structure in the time domain.

III. Results

A thin metal-clad silica rectangular waveguide with an air core and a thin layer of polysterene deposited at the inner surface of the metal cladding, as shown in Fig.1, has been considered as the structure of the multimode Interference coupler.

The complex refractive indices used for the gold (Au) metal-cladding, the silica outer cladding and polysterene inner coating where considered to be 281.55 + j419.74 [22], 1.96 + j0.0061 and 1.58 + j0.0036, respectively, at an operating frequency of 2.5 THz. A complex refractive index of 1.0 + j1*10^{-6} for air to take into account the loss at the above frequency, has been used. The height H_{MMM}, and the width, W_{MMI}, of the MMI structure were considered to be 1mm and 3 mm, respectively and the position of the input and output ports, spaced by a distance of half the MMI width along the horizontal direction, according to the self imaging principle, are also pointed in Fig.1. The metal thickness was considered to be 0.5 μm and the polysterene thickness was varied to achieve minimum modal loss.

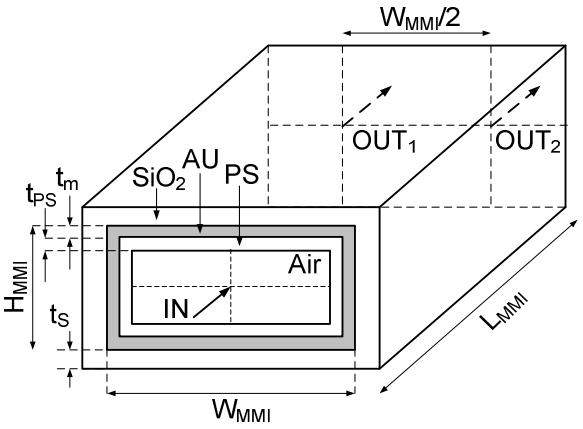

Fig.1. Hollow-core Polysterene-coated THz MMI

Intially, the fundamental and the first order higher TM modes of the MMI cross section, presented in Fig.2 have been obtained using the full vectorial H-field FEM and the propagation constants were found to be β_0 = 52.2424 mm^{-1} and β_1 = 52.2120 mm^{-1}, respectively, thus giving a self image length, L_i of 77.51 mm and consequently a half power length corresponding to the length of the MMI of L_{MMI} = 38.76 mm.

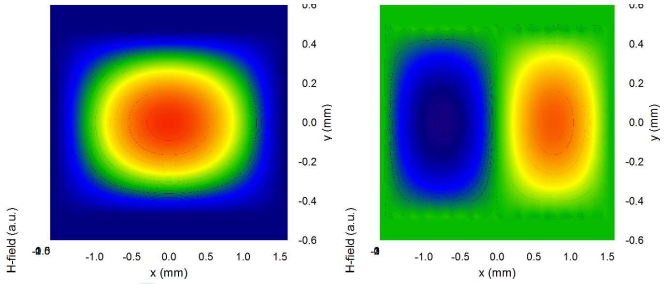

Fig.2. (a) Fundamental and (b) first order TM mode of the MMI

It should be noted that the MMI height has been designed to be 1mm to ensure single mode behaviour along the vertical dimension. The thickness of the inner polysterene coating has been varied and the complex propagation characteristics of the fundamental mode are presented in Fig.3.

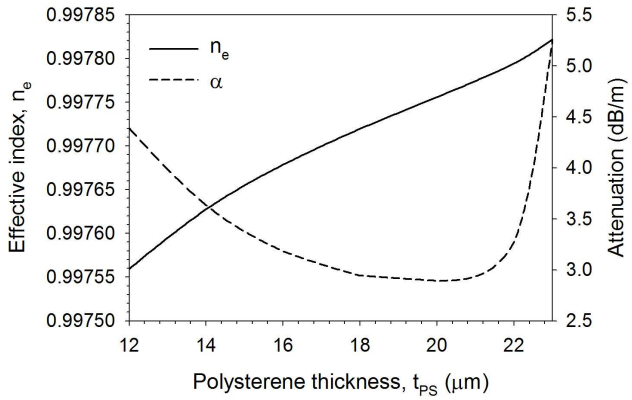

Fig.3. Propagation Characteristics of the fundamental mode of the MMI structure with the polysterene thickness, t_{PS}

As can be seen from the above characteristics the effective index increases with the increase of the polysterene thickness, for the range examined. However, the variation of the attenuation exhibits a minimum modal loss of about 3dB/m for a polysterene thickness of 20 μm, and therefore the above thickness has been selected as the optimum value in the design of the MMI structure. The accuracy of the FEM approach has been verified by considering a square structure of the same material and the same MMI width and height in both lateral dimensions of 1.8 mm, in which the polysterene thickness was varied. A minimum attenuation of 1.1dB/m has been obtained in the above structure, for a polysterene thickness of 15 μm. The above level of attenuation is found to be in fine agreement with the minimum transmission loss reported in [8] for the hybrid HE_{11} mode of a polysterene-lined hollow cylindrical metal waveguide, with a core diameter of 1.8 mm.

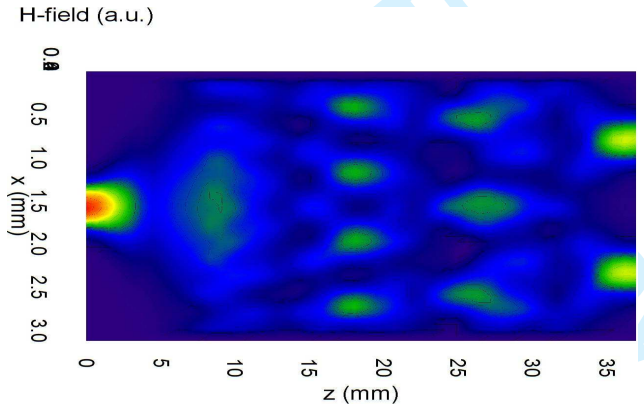

Fig.4 BPM Simulation of the MMI 3dB coupler

The FEM-BPM approach has then been used to demonstrate the optical field evolution along the direction of propagation of the MMI 3dB power splitter. The H-field evolution, obtained from a horizontal plane (x-axis) at the centre of the waveguide (half MMI height) along the direction of propagation (z-axis), for a Gaussian beam of a spot size diameter of 0.6 mm launched at the centre of the MMI (as shown in Fig.1), is presented in Fig.4. As can be seen from the above field evolution, multiple images of the input field are excited along the direction of propagation until the two half-images are obtained at a position of about 37.2 mm along the direction of propagation.

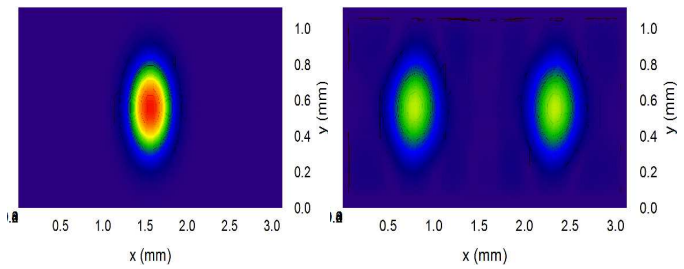

Fig.5 Input Gaussian beam and MMI output H-field

Although, there is a small difference from the device length estimated using the FEM approach, the position of the half-images can be varied with the spot-size diameter of the launched Gaussian beam, as presented in the following sections. However, within an MMI length span of 2 mm, the reduction of the field intensity does not drop below 3 % from the maximum intensity.

The field images of the Gaussian input at the cross-section of the input and output of the MMI device are also presented in Fig.5. The output images are half power replicas of the launched field and spaced along the centre of the MMI at a distance equal to half the MMI width, as expected.

Further, the performance of the MMI device in the time domain has been examined using the FDTD approach. Initially, a sinusoidal wave at 2.5 THz has been launched to demonstrate the performance of the device for a monochromatic source and the field evolution from a horizontal plane at the centre of the waveguide (as obtained in the FE-BPM approach) is presented in Fig.6

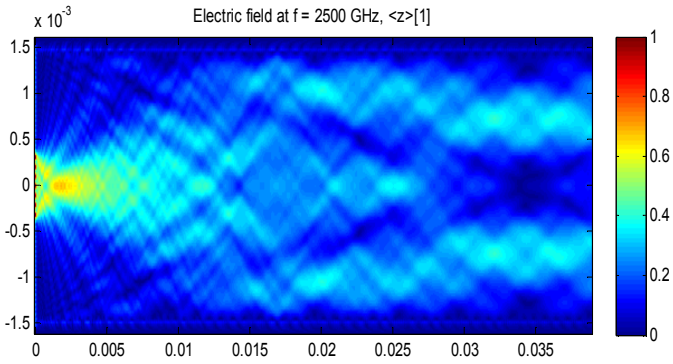

Fig.6 FDTD simulation of the MMI for a sinusoidal wave input at 2.5 THz.

In the above simulation, 4000 time steps have been used and by launching a sinusoidal wave with a spot-size diameter of 0.76 mm, the length of the device was found to be 38.8 mm, therefore, in fine agreement with the designed MMI length obtained using the modal solution of the FEM approach.

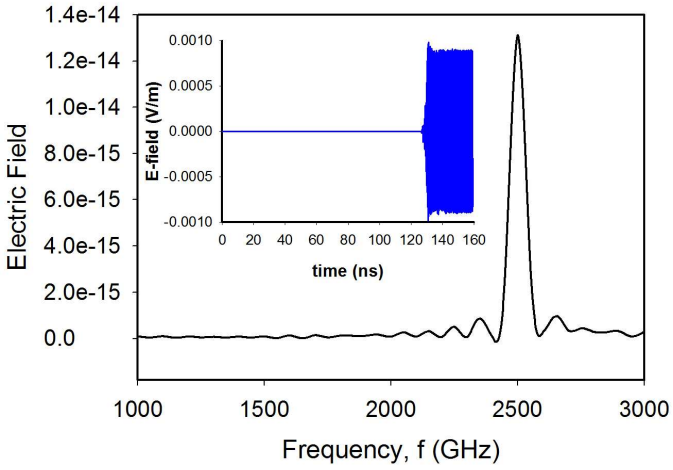

Fig.7 Frequency spectrum of the output sinusoidal wave (shown as inset) obtained from MMI output port 1.

The frequency spectrum of the output sinusoidal wave at the left port (assigned as port 1 in Fig.1) is presented in Fig. 7, where it can be seen that the maximum frequency is located at

2.5 THz as expected. The sinusoidal wave evolution along the direction of propagation is also shown as inset.

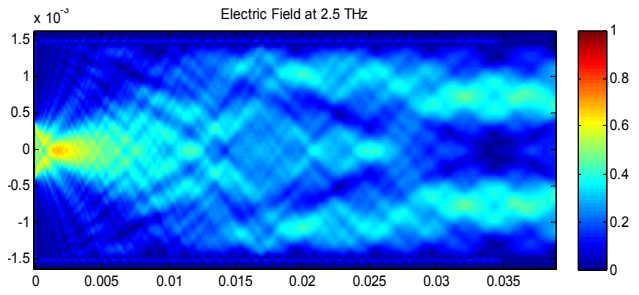

Fig.8 FDTD simulation of the MMI 3dB coupler for a Gaussian input.

Further, a Gaussian beam of spot-size diameter of 0.76 mm, launched the input of the MMI device has been simulated using the FDTD approach and the field evolution from a horizontal plane at the centre of the device, along the direction of propagation is presented in Fig. 8. The length of the device for the above spot-size diameter was found to be about 38.82 mm, in fine agreement with the length obtained from the FEM modal solution.

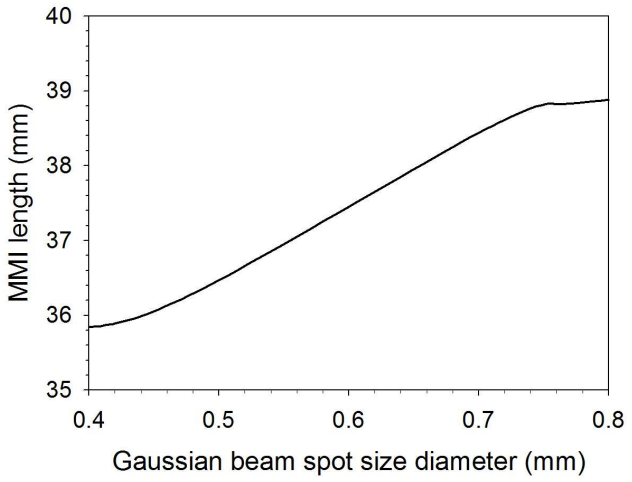

Fig.9 MMI Length with Gaussian input spot-size diameter.

As has been mentioned in the preceding sections, the MMI length can be optimized with the variation spot-size diameter of the beam source, as presented in Fig.9. In the above characteristics it can be seen that the MMI length increases linearly with the source spot-size diameter, for a certain range. By increasing further the spot-size diameter, the images at the output ports deteriorate (not shown here), since the spot-size is limited by the height of the device.

Finally, the Electric field, obtained from the left port output of the MMI device, from the Gaussian input beam of spot size diameter of 0.76 mm, examined in Fig.8, is presented in Fig.10. The waveguide dispersion parameter, D, of the device at 2.5 THz was estimated to be about 0.1 ps/(μm*m). This corresponds to pulse broadening of about 0.85 ps for a 0.038 m long waveguide and a bandwidth of 1.4 THz. The dispersion levels of the device is relatively small because the propagation is performed inside the air core and the mode is isolated from the surface modes propagating along the metal-dielectric interfaces of the structure due to the polysterene coating. The dispersion level is also found to be in good agreement with the dispersion presented in [23] for a structure with circular geometry.

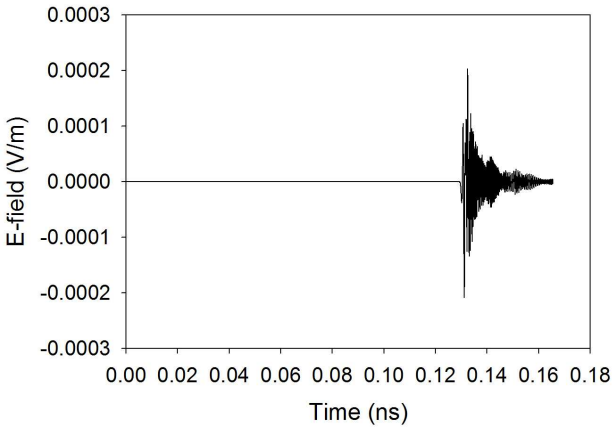

Fig.10 Output H-field with time at port 1 for Gaussian input.

IV. Conclusion

Finite element and finite difference based approaches in space and time have been used to demonstrate, for the first time to our knowledge, the performance of a hollow core polysterene-coated metallic waveguide-based multimode interference half power coupler for THz wave propagation. The transmission losses and the dispersion levels have been found to in agreement with previous published work.

References

[1] R H Jacobson, D M Mittleman, and M C Nuss, 'Chemical recognition of gases and gas mixtures with terahertz waves,' *Optics Lett.*, **21**, pp.2011-2013, 1996.

[2] Q Chen, Z Jiang, G X Xu, and X C Zhang, 'Near-field terahertz imaging with a dynamic aperture,' *Optics Lett.*, **25**, pp.1122-1124, 2000.

[3] J Zhang and D Grischkowsky, 'Waveguide terahertz time-domain spectroscopy of nanometer wave layers,' *Optics Lett.*, **29**, pp.1617-1619, 2004.

[4] R Kohler, A Tredicucci, F Beltram, H E Beere, E H Linfield, A G Davies, D A Richie, R C Iotti, and F Rossi, 'Terahertz semiconductor-heterostructure laser,' *Nature*, **417**, pp.156-159, 2002.

[5] J. A. Harrington, R. George, P. Pedersen, and E. Mueller, "Hollow polycarbonate waveguides with inner Cu coatings for delivery of terahertz radiation," *Opt. Exp.*, vol. 12, pp. 5263–5268, 2004.

[6] C.-H. Lai, Y.-C. Hsueh, H.-W. Chen, Y. J. Huang, H. C. Chang, and C. K.Sun,"Low-index terahertz pipe waveguides," *Opt. Lett.*, vol. 34, pp. 3457–3459, 2009.

[7] D. Chen and H. Chen, "A novel low-loss Terahertz waveguide: Polymer tube," *Opt. Exp.*, vol. 18, pp. 3762–3767, 2010.

[8] O. Mitrofanov, R. James, F. A. Fernández, T. K. Mavrogordatos, and J. A. Harrington, "Reducing Transmission Losses in Hollow THz Waveguides" IEEE Trans. on THz Sci. and Technol., vol.1,pp.124-132, 2011

[9] B. M. A. Rahman, A. Quadir, H. Tanvir, and K. T. V. Grattan, Characterization of Plasmonic Modes in a Low-Loss Dielectric-Coated Hollow Core Rectangular Waveguide at Terahertz Frequency," *IEEE Photonics J.*, vol.3, No.6, pp., 2011.

[10] T. Rasmussen, J.K. Rasmussen and J.H. Povlsen, "Design and performance evaluation of 1-by-64 multimode interference power splitter for optical communications," J. Lightwave Technol. **13**, pp. 2069-2074, 1995.

[11] C.G.P. Herben, C.G.M. Vreeburg, X.J.M. Leijtens, H. Blok, F.H. Groen, I. Moerman, J.W. Pedersen and M.K. Smit, "Chirping of an MMI-PHASAR Demultiplexer for application in multiwavelength laser," IEEE Photonics Technol. Lett. **9**, pp.1116-1118, 1997.

[12] R.J. Deri, E.C.M. Pennings, A. Scherer, A.S. Gozdz, C. Caneau, N. Andreadakis, V. Shah, L. Curtis, R.J. Hawkins, J.B.D. Soole and J.I. Song, "Ultracompact monolithic integration of balanced, polarization diversity photodetectors for coherent lightwave receivers," IEEE Photonics Technol. Lett. **4**, pp.1238-1240, 1992.

[13] L.B. Soldano, A.H de Vreede, M.K. Smit, B.H. Verbeek, E.G. Metaal and F.H. Groen, "Mach-Zehnder interferometer polarization splitter in InGaAsP/ InP," IEEE Photonics Technol. Lett. **6**, 402-405, 1994.

[14] B.M.A. Rahman and J.B. Davies, "Finite-element solution of integrated optical waveguides," J. Lightwave Technol. **2**, 682-688 (1984).

[15] C. Themistos, B.M.A. Rahman and K.T.V. Grattan, "Finite element analysis for lossyy optical waveguides by using perturbation techniques, *IEEE Photon. Technol. Lett*., vol.6, pp.537-539., 1994.

[16] M.D. Feit and J.A. Fleck, "Light propagation in graded-index optical fibers," *Appl. Opt*., 17, pp.3990-3998, 1978

[17] Y. Tsuji, M. Koshiba and T. Tanabe, "A wide-angle- beam propagation method based on a finite element scheme," IEEE Trans. Magnetics, **33**, pp.1544-1547, 1997.

[18] S. S. A. Obayya, B. M. A. Rahman and H. A. El-Mikati, "New Full-Vectorial Numerically Efficient Propagation Algorithm Based on the Finite Element Method," *J. Lightwave Technol*., vol.**18**, no.3, pp.409-415, 2000

[19] A. Taflove and S. C. Hagness, *Computational electrodynamics : the finite-difference time-domain method*, 3rd ed. Boston: Artech House, 2005.

[20] J.-P. Berenger, "A perfectly matched layer for the absorption of electromagnetic waves," *J. Comput. Phys.,* vol. 114, pp. 185-200, 1994.

[21] C. Themistos, B. M. A. Rahman, M. Rajarajan, K. T. V. Grattan, B. Bowden, and J. Harrington, BCharacterization of Silver/Polystyrene (PS)-coated hollow glass waveguides at THz frequency,[J. Lightw. Technol., vol. 25, no. 9, pp. 2456–2462, 2007.

[22] M. Ordal, L. Long, R. Bell, S. Bell, R. Bell, R. Alexander, and C. Ward, BOptical properties of the metals Al, Co, Cu, Au2Fe, Pb, Ni, Pd, Pt, Ag, Ti, and W in the infrared and far infrared,[Appl. Opt., vol. 22, no. 7, pp. 1099–1120, 1983.

[23] Oleg Mitrofanov and James A. Harrington, "Dielectric-lined cylindrical metallic THz waveguides: mode structure and dispersion", Optics Express, vol. 18, No.3, pp. 1898-, Feb 2010.

C. Markides (biography and photograph are not available at the moment).

C. Themistos (biography and photograph are not available at the moment).

H. Tanvir (biography and photograph are not available at the moment).

B.M.A. Rahman (biography and photograph are not available at the moment)

K.T.V. Grattan (biography and photograph are not available at the moment)

List of Authors

Markides / Christos / Mr / Department of Computer Science and Engineering, School of Engineering and Applied Sciences / Frederick University, 7 Y. Frederickou, Palouriotissa, Nicosia 1036, Cyprus,/ Tel. +357-22431355 / Fax.: +357-22438234 / E-mail: cmarkides@cmarkides.info

Themistos / Christos / Dr / Electrical Engineering Department, School of Engineering and Applied Sciences / Frederick University, 7 Y. Frederickou, Palouriotissa, Nicosia 1036, Cyprus,/ Tel. +357-22431355 / Fax.: +357-22438234 / E-mail: c.themistos@cytanet.com.cy

Tanvir / Huda / Dr / Department of Engineering and Mathematical Sciences, City University, Northampton Square, London EC1V 0HB, UK/ Tel.: +44 (0)20 7040 8123 Fax: +44 (0)20 7040 8568, e-ail: H.Tanvir@city.ac.uk).

Rahman / B. M. Azizur / Professor / Department of Engineering and Mathematical Sciences, City University, Northampton Square, London EC1V 0HB, UK/ Tel.: +44 (0)20 7040 8123 Fax: +44 (0)20 7040 8568, b.m.a.rahman@city.ac.uk

Grattan / Kenneth T. V. / Professor / Department of Engineering and Mathematical Sciences, City University, Northampton Square, London EC1V 0HB, UK/ Tel.: +44 (0)20 7040 8121 Fax: +44 (0)20 7040 8121